Diagn Interv Radiol 2018; 24:262-267



INTERVENTIONAL RADIOLOGY

ORIGINAL ARTICLE

# Usefulness of fusion images of unenhanced and contrast-enhanced arterial phase cone-beam CT in the detection of viable hepatocellular carcinoma during transarterial chemoembolization

Eu Hyun Kim
Jung Suk Oh
Ho Jong Chun
Byung Gil Choi
Hae Giu Lee

**PURPOSE**
We aimed to evaluate the diagnostic efficacy of fusion imaging of unenhanced and arterial phase contrast-enhanced cone-beam computed tomography (CBCT) by comparing with multidetector computed tomography (MDCT) in detection of viable hepatocellular carcinoma (HCC) in patients who have been previously treated with transarterial chemoembolization (TACE).

**METHODS**
In this retrospective study, a total of 173 tumors in 33 known HCC patients (21 men, 12 women; mean age, 64±7.6 years; mean tumor size, 2.15±1.70 cm) who had been previously treated with TACE and underwent additional session of TACE were included. The sensitivity and positive predictive values of preprocedural MDCT and fusion CBCT for detection of viable tumor were analyzed with follow-up MDCT images performed 3-4 weeks after TACE, as reference standard.

**RESULTS**
A total of 141 remote and 32 marginal viable tumors were included. The sensitivities for detection of remote, marginal, and total viable tumors were 80.9%, 68.8%, and 78.6% for MDCT and 96.5%, 96.9%, and 96.5% for fusion CBCT, respectively. The positive predictive values for detection of remote, marginal, and total viable tumors were 95.0%, 78.6%, and 95.8% for MDCT, and 97.1%, 88.6%, and 97.7% for fusion CBCT, respectively. Fusion CBCT showed statistically higher sensitivity and positive predictive value for detection of viable tumors ($P < 0.001$).

**CONCLUSION**
The diagnostic performance of fusion imaging of unenhanced and contrast-enhanced arterial phase CBCT was superior to MDCT for detection of viable HCCs.

Transarterial chemoembolization (TACE) is one of the well-established and widely performed treatments for hepatocellular carcinoma (HCC), especially in patients with intermediate or advanced stage tumors without operability (1–3). This procedure consists of intraarterial administration of chemotherapeutic agent as well as ethiodized oil, and the degree of uptake of ethiodized oil after TACE is thought to represent tumor necrosis and imply the patient's prognosis (1, 2).

TACE is often not completed in a single session due to residual or recurrent tumors, necessitating repeated TACE. Thus, follow-up for detection of new or remaining viable tumor is important. In general, computed tomography (CT), particularly multidetector computed tomography (MDCT) is the modality of choice for surveillance. Analyzing attenuation difference between the arterial and unenhanced phases of CT scans is the most commonly used method to evaluate viable tumor in ethiodized oil-laden HCCs (4). However, detection of subtle arterial enhancement adjacent to or inside a retained ethiodized oil nodule may be difficult because the retained ethiodized oil nodule shows high attenuation on all phase images (4, 5). The beam hardening artifact and volume averaging effects around retained ethiodized oil make detection of the true arterial enhancement difficult (3). To overcome this difficulty, many attempts have been made to help better depiction of viable tumors around the tumors with ethiodized oil accumulation, including utilization of $^{18}$F-FDG PET-CT, magnetic resonance imaging (MRI), dual-energy CT analysis with advanced postprocessing, and contrast-enhanced ultrasonography (2, 3, 6–8).

From the Department of Radiology (J.S.O. ✉ *oj-cumc@daum.net*), Seoul St. Mary's Hospital, The Catholic University of Korea College of Medicine, Seoul, Republic of Korea.

Received 20 December 2017; revision requested 18 January 2018; last revision received 16 March 2018; accepted 30 March 2018.

DOI 10.5152/dir.2018.17503

You may cite this article as: Kim EH, Oh JS, Chun HJ, Choi BC, Lee HG. Usefulness of fusion images of unenhanced and contrast-enhanced arterial phase cone-beam CT in the detection of viable hepatocellular carcinoma during transarterial chemoembolization. Diagn Interv Radiol 2018; 24:262-267.

More recently, intraprocedural cone-beam CT (CBCT) has been recognized to be an effective and valuable tool for detection of subtle enhancing portion in many interventional procedures including TACE (1, 9–13). However, in a single-phase CBCT there is a limit to distinguish between true arterial enhancing nodules and retained ethiodized oil nodules because both are seen as hyperattenuating nodules. In order to improve the diagnostic and therapeutic performance in patients who had been treated with TACE, intraprocedural dual-phase CBCT and fusion images created from the CBCT images could be utilized for detection of remnant or recurrent viable tumor.

The aim of this study is to evaluate the diagnostic effectiveness of fusion imaging of unenhanced and contrast-enhanced cone-beam computed tomography (CBCT) compared with MDCT in detection of viable tumor in HCC patients previously treated with transarterial chemoembolization (TACE).

## Methods

### Patient selection

This retrospective study was Institutional Review Board-approved and the informed consent was waived due to the retrospective nature. Between February and July 2016, 240 consecutive HCC patients, who had been previously treated with TACE, underwent additional TACE. Among these patients, only patients meeting the following criteria were included in this study: 1) Follow-up MDCT was performed within 1 month before the additional TACE and the exam showed retained ethiodized oil nodules; 2) Recurrent viable HCCs, defined by arterial enhancement and delayed washout on MDCT scan with elevated level of serum tumor markers, were present without macroscopic vascular invasion or portal vein thrombosis. The exclusion criteria were: 1) tumor size <0.5 cm (n=94); 2) infiltrative tumor with immeasurable extent (n=24); 3) >1 month interval between MDCT and TACE (n=21); 4) no evidence of retained ethiodized oil nodule on follow-up MDCT (n=68).

Among 240 consecutive patients, 207 patients were excluded, and a total of 33 patients (21 men and 12 women; mean age, 64±7.6 years) with 173 recurrent HCC nodules (mean tumor size, 2.15±1.70 cm; range, 0.5–10.6 cm) were included in this study. Although none of the tumors included in this study was histopathologically confirmed, all patients met the generally used clinical and imaging diagnostic criteria of HCC. Postprocedural unenhanced CBCT and the follow-up MDCT after 3-4 weeks were regarded as reference standards. The patient's medical records and radiology reports were also retrospectively reviewed. The basic characteristics of the included patients are summarized in Table 1.

### CT examinations

All patients underwent quadruple-phase MDCT (unenhanced, arterial, portal venous, delayed phases) before and after TACE. MDCT images were obtained using a 64-row helical CT scanner) (SOMATOM Definition, Siemens Medical Solutions) with the following scanning protocol: tube voltage, 80–100 kVp; beam collimation, 14×1.2 mm; pitch, 0.6; tube current product value, 180 mAs; rotation time, 0.5 s. An arterial phase scan was taken using the bolus tracking method (scanning starting after an 8 s delay from the time when the region of interest in the aorta exceeded 150 HU) with iodine contrast medium (ioversol, 350 mg iodine/mL; Optiray 350, Tyco Healthcare). Then, portal and delayed phase scans were obtained at 30 s and 120 s after beginning the arterial phase scan, respectively. Follow-up CT scan was performed 3-4 weeks after TACE to evaluate the therapeutic effect.

### Cone-beam CT acquisition, fusion, and TACE technique

All procedures were performed by two experienced interventional radiologists (6 years and 14 years of experience post-fellowship, respectively) in an interventional radiology suite equipped with angiography system (AlluraClarity FD20, Philips) and CBCT (XperCT, Philips Healthcare). Fusion image requires registration of dual-phases of three-dimensional (3D) rotational CBCT data sets, i.e., unenhanced and arterial. The system's isocenter was positioned over the area of interest and a total of 312 projection images (60 frames per second) were acquired for 5.2 s with a motorized C-arm that covered a 240° clockwise arc at a rotation speed of 55° per second during a breath-hold. Initial

**Main points**

- Determination of marginal viable tumor around retained ethiodized oil is not easy, since subtle arterial enhancement should be detected adjacent to or inside a retained ethiodized oil nodule, which is hyperdense itself.
- The beam hardening artifact and volume averaging effects around retained ethiodized oil make detection of the true arterial enhancement even more difficult.
- Fusion imaging of unenhanced and contrast-enhanced arterial phase CBCT is a valuable tool to aid detection of viable tumors in patients undergoing repeated TACE.
- The results of current study revealed superiority of CBCT over MDCT in detection of HCC after TACE.

**Table 1.** Patient characteristics

| | |
|---|---|
| Age (years), mean±SD (range) | 64±7.6 (47–80) |
| Sex (M:F) | 21:12 |
| Cause of cirrhosis and HCC, n | |
| Hepatitis B-related cirrhosis | 22 |
| Hepatitis C-related cirrhosis | 7 |
| Alcoholic cirrhosis | 3 |
| Cryptogenic | 1 |
| Child-Pugh score, n | |
| A | 28 |
| B | 5 |
| C | 0 |
| Number of previous TACE session, mean±SD (range) | 5.3±2.4 (2–14) |

SD, standard deviation; M, male; F, female; HCC, hepatocellular carcinoma; TACE, transarterial chemoembolization.

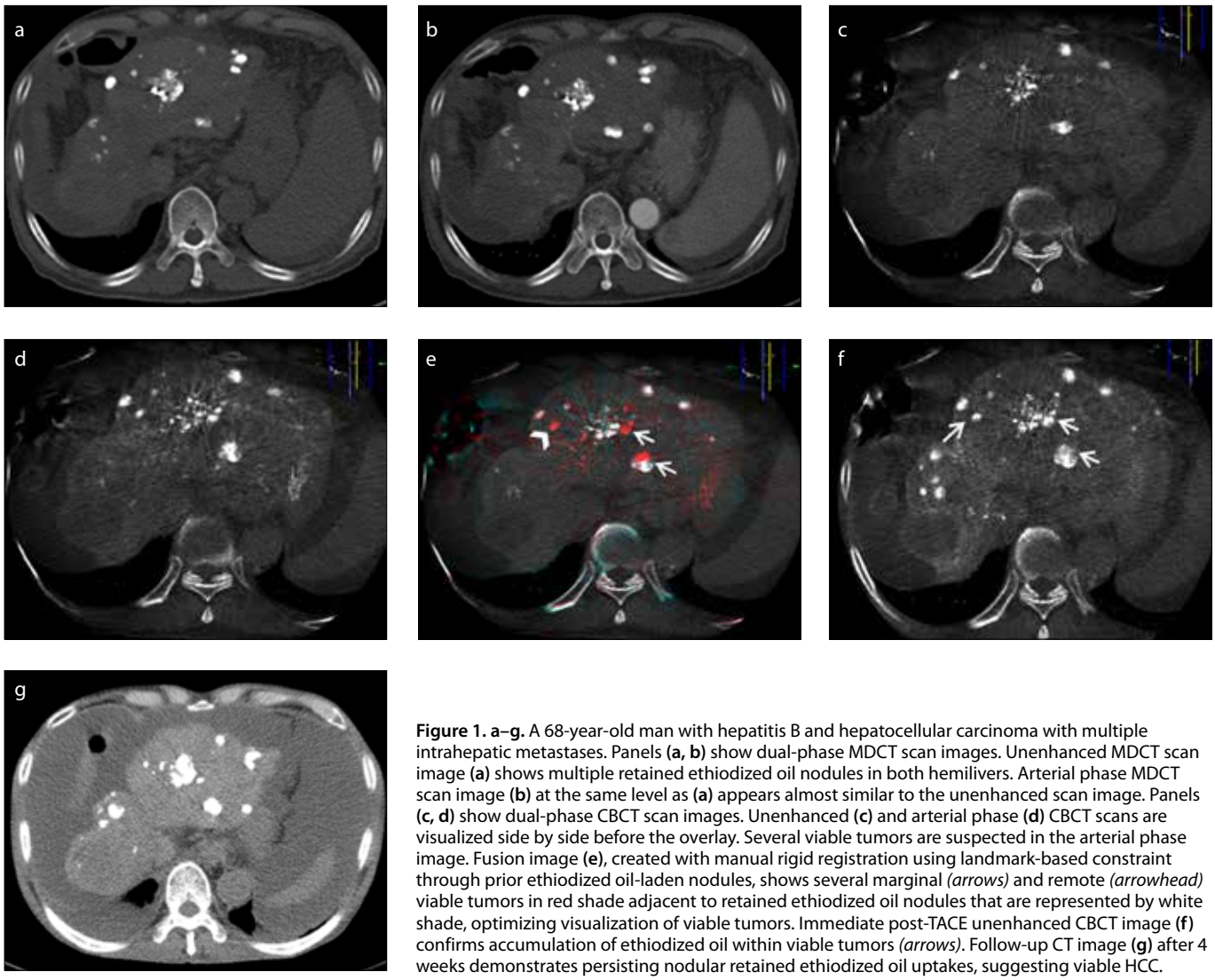


**Figure 1. a–g.** A 68-year-old man with hepatitis B and hepatocellular carcinoma with multiple intrahepatic metastases. Panels **(a, b)** show dual-phase MDCT scan images. Unenhanced MDCT scan image **(a)** shows multiple retained ethiodized oil nodules in both hemilivers. Arterial phase MDCT scan image **(b)** at the same level as **(a)** appears almost similar to the unenhanced scan image. Panels **(c, d)** show dual-phase CBCT scan images. Unenhanced **(c)** and arterial phase **(d)** CBCT scans are visualized side by side before the overlay. Several viable tumors are suspected in the arterial phase image. Fusion image **(e)**, created with manual rigid registration using landmark-based constraint through prior ethiodized oil-laden nodules, shows several marginal *(arrows)* and remote *(arrowhead)* viable tumors in red shade adjacent to retained ethiodized oil nodules that are represented by white shade, optimizing visualization of viable tumors. Immediate post-TACE unenhanced CBCT image **(f)** confirms accumulation of ethiodized oil within viable tumors *(arrows)*. Follow-up CT image **(g)** after 4 weeks demonstrates persisting nodular retained ethiodized oil uptakes, suggesting viable HCC.

CBCT was performed without contrast injection. For the second CBCT, after placing a 5 F catheter in the common or proper hepatic artery, the contrast medium (Visipaque 270, GE Healthcare) was injected using a power injector at a rate of 1.5 or 2 mL/s for 12 s (for a total of 18 or 24 mL) and image acquisition was performed after an 8 s delay.

The acquired images were immediately transferred to a 3D workstation (PhillipsAlluraXtraVision 8.3), in parallel to acquiring data for volume reconstruction. Two volumes (unenhanced and arterial phases) were visualized side by side for the overlay and were manually registered. Image fusion was accomplished with manual rigid registration using landmark-based constraints through adjacent vessel wall calcifications, bony structures, and prior ethiodized oil uptakes (Fig. 1).

After target tumors for treatment were decided with the aid of the fusion image, TACE was conducted in the usual standard fashion by superselective catheterization of the tumor feeding vessels with a microcatheter, followed by infusion of ethiodized oil (Lipiodol; Andre Guerbet) and doxorubicin hydrochloride (Adriamycin RDF; Ildong Pharmaceutical) emulsion. Additional embolization was performed with 150 to 300 μm sized calibrated gelatin sponge particles (Cali-Gel; Alicon). At the end of the procedure, completion unenhanced CBCT was scanned with the same protocol. Completion CBCT image was performed without enhancement and was again fused with unenhanced CBCT image with manual rigid registration.

### Image analysis

Three radiologists with 4, 7, and 15 years of clinical experience in abdominal imaging who did not participate in the TACE procedures independently interpreted each patient's MDCT images. All radiologists were blinded to the number and location of the tumors. The fusion images were stored as DICOM files and sent to Picture Archiving and Communications System (PACS; Maroview, version 5.4, Infinite) and represented in monitors of a spatial resolution of 1600×1200. Disagreements were resolved by consensus.

Viable HCCs were divided into two types, namely marginal or remote. On MDCT, manual marking and recording of location and number of the viable tumors were made by abdominal radiologists. A marginal viable HCC was defined as a nodule with ethiodized oil retention hyperattenuating or isoattenuating on arterial phase and as hypoattenuating or isoattenuating on delayed phase. Presence of remote viable tumor was evaluated based on nodular arterial enhancement with delayed washout. On fusion CBCT, true arterial enhancement was clearly distinguished by masking the

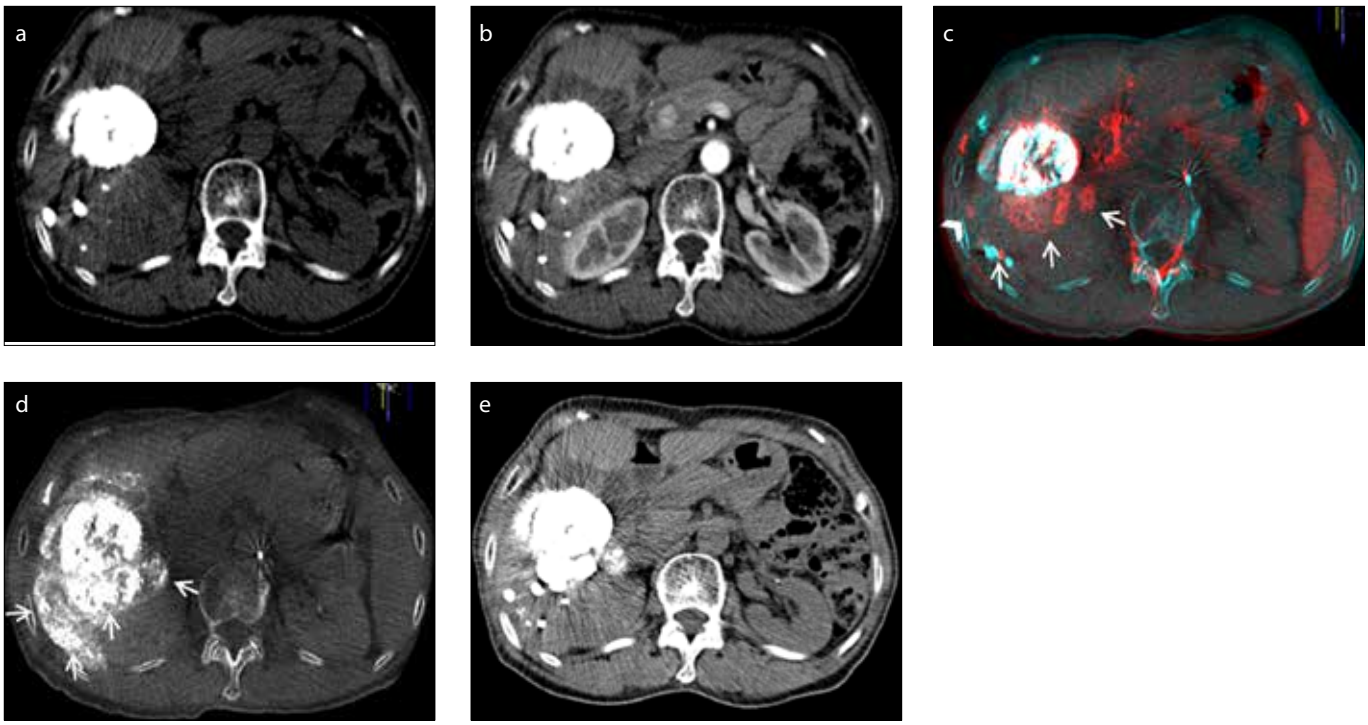


**Figure 2. a–e.** A 73-year-old man with hepatitis B and hepatocellular carcinoma. On unenhanced **(a)** and arterial phase **(b)** MDCT scan images, there is large and compact retained ethiodized oil mass as well as a few smaller treated tumors in the right hemiliver. When comparing these two images, there is no definite discernable viable tumor. Note the severe beam-hardening artifact caused by the large previously treated tumor; this might obscure detection of adjacent viable tumors. Fusion image **(c)**, created with manual rigid registration using landmark-based constraint through prior ethiodized oil-laden nodules, shows several marginal *(arrows)* and remote *(arrowhead)* viable tumors in red shade adjacent to retained ethiodized nodules that are represented by white shade, optimizing visualization of viable tumors despite beam hardening artifact. Immediate post-TACE unenhanced CBCT image **(d)** confirms accumulation of ethiodized oil within viable tumors *(arrows)*. Follow-up CT **(e)** after 4 weeks demonstrates persisting nodular ethiodized oil uptakes, suggesting viable HCC.

unenhanced attenuation from the arterial attenuation: hyperattenuating lesion of primary CBCT scan image (arterial phase) was represented with red shade and hyperattenuating lesion of overlay scan image (unenhanced phase) was expressed as blue shade. After image fusion was created, true arterial enhancing nodules were represented by intense red shade while ethiodized oil-laden nodule was represented by white-blue shade, meaning the blue shade of the unenhanced phase scan overlaid by white shade of the ethiodized oil itself. Subtle arterial enhancement adjacent to the retained ethiodized oil is expected to be clearly seen, because the retained ethiodized oil attenuation is not accentuated in fusion CBCT. A marginal viable HCC in the retained ethiodized oil nodule was defined as any nodular or circumferential tumor of red shade within the white background of partial uptake of retained ethiodized oil (Fig. 2). Remote viable tumor was expressed as nodular red shade.

For reference standard, comparison of pre- and immediate post-TACE unenhanced CBCT images was performed for presence of new ethiodized oil uptake, as well as follow-up MDCT images performed after 3-4 weeks after the TACE. The newly noted nodular ethiodized oil uptakes on follow-up CBCT were considered as viable tumor, if it was also seen on the follow-up MDCT.

### Statistical analysis

The sensitivity and positive predictive values for detecting HCC per tumor were calculated. Comparison of MDCT and fusion CBCT were done using the McNemar test for sensitivity and positive predictive values. A $P$ value < 0.05 was considered to indicate a statistically significant difference. Computer software packages (SPSS 12.0 for Windows, SPSS) were used for statistical analysis.

## Results

The mean numbers of previous TACE session that patients underwent were 5.3±2.4 (range, 2–14). There were 141 remote viable tumors and 32 marginal viable tumors that located around the previously retained ethiodized oil nodules. The median time interval from baseline preprocedural MDCT to additional TACE was 1 day (range, 0–29 days).

The diagnostic performance of MDCT and fusion CBCT are presented by the sensitivity and positive predictive value per tumor in Table 2. The sensitivity of total viable HCC detection was 96.5% (167/173) in fusion CBCT and 78.6% (136/173) in MDCT with significant statistical difference. When HCC was categorized into two groups as remote and marginal viable tumors, fusion CBCT showed significantly higher sensitivity for detection of both groups ($P$ < 0.001); sensitivity was 96.5% (136/141) in fusion CBCT vs. 80.9% (114/141) in MDCT for remote viable tumors ($P$ < 0.001) and 96.9% (31/32) in fusion CBCT vs. 68.8% (22/32) in MDCT for marginal viable tumors ($P$ = 0.001).

The overall positive predictive values for detection of remote, marginal, and total viable tumors were 97.1%, 88.6%, and 97.7% for CBCT, and 95.0%, 78.6%, and 95.8% for MDCT, respectively. Positive predictive values differed between the two groups ($P$ < 0.001).

## Discussion

With the advance of imaging modalities and techniques, treatment for HCC is also developing, with TACE on the forefront.

**Table 2.** Diagnostic performance for detection of remote or marginal HCC after TACE on MDCT and CBCT

| | Sensitivity | | | Positive predictive value | | |
|---|---|---|---|---|---|---|
| | MDCT | CBCT | *P* | MDCT | CBCT | *P* |
| Remote | 80.9% (114/141) | 96.5% (136/141) | <0.001 | 95.0% (114/120) | 97.1% (136/140) | <0.001 |
| Marginal | 68.8% (22/32) | 96.9% (31/32) | 0.001 | 78.6% (22/28) | 88.6% (31/35) | 0.001 |
| Total | 78.6% (136/173) | 96.5% (167/173) | <0.001 | 95.8% (136/142) | 97.7% (167/171) | <0.001 |

HCC, hepatocellular carcinoma; TACE, transarterial chemoembolization; MDCT, multidetector computed tomography; CBCT, cone-beam computed tomography.

Especially, utilization of CBCT has greatly improved both sensitivity and specificity in detection of HCC, has provided information about tumor feeders enabling superselective TACE, and has been used to predict therapeutic response (1, 9–13). The benefit of acquisition of dual-phase CBCT consisting of early arterial and delayed venous scans is well known and undoubted despite additional radiation exposure caused by performing CBCT, as it enables reduction of extra X-ray dose caused by repeated digital subtraction angiography (DSA) (10). Above all, CBCT during hepatic arteriography demonstrated a high tumor-to-background contrast as contrast material is locally administered (12), being sufficient for detection of almost all small HCC tumors (14).

Although new technologies have increased the technical success rate of TACE (13), repeated TACE is inevitable due to residual or recurrent tumors. Detection of viable tumor in patients who have previously undergone TACE is troublesome and time-consuming, since dense ethiodized oil makes it hard to distinguish adjacent arterial enhancement. Consequently, many studies in the literature have reported various means to determine viability of tumors with ethiodized oil accumulation (2, 3, 6–8).

The reported sensitivity and positive predictive value of CBCT in depiction of HCC during TACE are 90% (range, 82%–95%) and 89% (74%–96%), respectively (15). In a study performed by Iwazawa et al. (16), which compared the diagnostic performance of MDCT and CBCT, the overall sensitivity for detection of HCC was significantly higher with CBCT (85.9%) than MDCT (61.9%). The overall positive predictive value was higher with MDCT (92.8%) than CBCT (88.9%), yet the difference was statistically insignificant. These previous studies included initially diagnosed HCCs, unlike the current study which focuses on marginal and remote recurrent/remnant HCCs. The results of this study is comparable in that fusion CBCT (96.5%) showed superiority in sensitivity over MDCT (78.6%), but different in that higher positive predictive value was noted in fusion CBCT (97.7%) compared with MDCT (95.8%).

The results of this study showed that fusion image is better than conventional MDCT in depicting viable HCC, in terms of sensitivity and positive predictive values, with statistical significance. By overlaying the early arterial CBCT images on unenhanced CBCT images, an operator can obtain images with improved conspicuity and does not have to conduct a direct visual comparison by simultaneously displaying the two phases side by side with scroll through the slices (17), thereby reducing the error of missing a viable tumor and facilitating to set a better treatment plan. In addition, time required for fusion imaging only takes a few minutes for a skillful user and application of fusion imaging is expected to be time-saving, especially for complex cases.

This study has several limitations. First, as this is a retrospective study, selection bias seems unavoidable. Second, tumors that are less than 0.5 cm in size and infiltrative in nature were not included in this study. Further investigations including these tumors could be conducted to prove the usefulness of fusion image. Third, misregistration could occur if a patient moves or breathes differently while undergoing unenhanced and contrast-enhanced CBCT and this could affect the diagnostic accuracy of the fusion images. Future investigations may be improved in terms of accuracy by introduction of software that registers unenhanced and contrast-enhanced CBCT images automatically and accurately. Fourth, one might argue about the image quality and radiation exposure of CBCT. CBCT has lower contrast resolution yet higher spatial resolution compared with MDCT, thus it provides sufficiently good image to aid TACE procedure (18). Tumor-feeding branches can be detected using specialized software utilizing CBCT images without selective angiography. Previous studies demonstrated that the procedural time and number of DSA could be decreased by using CBCT (15, 19). Furthermore, along with technical advancement, recently developed CBCTs enable acquisition of images with sufficient quality at the expense of reduced radiation exposure (20). Finally, for the detection of recurrent HCC, contrast-enhanced MRI and diffusion-weighted MRI may also be used, and these modalities have demonstrated promising results (21, 22). Previous studies have demonstrated superiority of MRI over MDCT in detecting tumor recurrence after TACE (23, 24), but how these techniques compare to the imaging method used in this study is not known. Further studies including both modalities are needed to clarify these issues.

In conclusion, the diagnostic performance of fusion imaging of unenhanced and contrast-enhanced arterial phase CBCT was superior to MDCT in the current study, in terms of sensitivity and positive predictive value for detection of both remote and marginal viable tumors. Therefore, fusion imaging can be used as a practical tool to detect recurrent viable tumors in HCC patients previously treated with TACE.

## Conflict of interest disclosure

The authors declared no conflicts of interest.

## References


1. Iwazawa J, Ohue S, Kitayama T, Sassa S, Mitani T. C-arm CT for assessing initial failure of iodized oil accumulation in chemoembolization of hepatocellular carcinoma. AJR Am J Roentgenol 2011; 197:W337–342. [CrossRef]
2. Kim SH, Lee WJ, Lim HK, Lim JH. Prediction of viable tumor in hepatocellular carcinoma treated with transcatheter arterial chemoembolization: usefulness of attenuation value measurement at quadruple-phase helical computed tomography. J Comput Assist Tomogr 2007; 31:198–203. [CrossRef]
3. Lee DH, Lee JM, Klotz E, et al. Detection of recurrent hepatocellular carcinoma in cirrhotic liver after transcatheter arterial chemoembolization: value of quantitative color mapping of the arterial enhancement fraction of the liver. Korean J Radiol 2013; 14:51–60. [CrossRef]

4. Kim HC, Kim AY, Han JK, et al. Hepatic arterial and portal venous phase helical CT in patients treated with transcatheter arterial chemoembolization for hepatocellular carcinoma: added value of unenhanced images. Radiology 2002; 225:773–780. [CrossRef]
5. Willatt JM, Hussain HK, Adusumilli S, Marrero JA. MR Imaging of Hepatocellular Carcinoma in the Cirrhotic Liver: Challenges and Controversies. Radiology 2008; 247:311–330. [CrossRef]
6. Lee JA, Jeong WK, Kim Y, et al. Dual-energy CT to detect recurrent HCC after TACE: initial experience of color-coded iodine CT imaging. Eur J Radiol 2013; 82:569–576. [CrossRef]
7. Cho YZ, Park SY, Choi EH, et al. The usefulness of contrast-enhanced ultrasonography in the early detection of hepatocellular carcinoma viability after transarterial chemoembolization: pilot study. Clin Mol Hepatol 2015; 21:165–174. [CrossRef]
8. Song HJ, Cheng JY, Hu SL, Zhang GY, Fu Y, Zhang YJ. Value of 18F-FDG PET/CT in detecting viable tumour and predicting prognosis of hepatocellular carcinoma after TACE. Clin Radiol 2015; 70:128–137. [CrossRef]
9. Ishikawa T, Abe S, Hoshii A, et al. Cone-beam computed tomography correlates with conventional helical computed tomography in evaluation of lipiodol accumulation in HCC after chemoembolization. PLoS One 2016; 11:e0145546. [CrossRef]
10. Higashihara H, Osuga K, Onishi H, et al. Diagnostic accuracy of C-arm CT during selective transcatheter angiography for hepatocellular carcinoma: comparison with intravenous contrast-enhanced, biphasic, dynamic MDCT. Eur Radiol 2012; 22:872–879. [CrossRef]
11. Kim HC. Role of C-arm cone-beam CT in chemoembolization for hepatocellular carcinoma. Korean J Radiol 2015; 16:114–124. [CrossRef]
12. Meyer BC, Frericks BB, Voges M, et al. Visualization of hypervascular liver lesions During TACE: comparison of angiographic C-arm CT and MDCT. AJR Am J Roentgenol 2008; 190:W263–269. [CrossRef]
13. Yu MH, Kim JH, Yoon JH, et al. Role of C-arm CT for transcatheter arterial chemoembolization of hepatocellular carcinoma: diagnostic performance and predictive value for therapeutic response compared with gadoxetic acid-enhanced MRI. AJR Am J Roentgenol 2013; 201:675–683. [CrossRef]
14. Miyayama S, Matsui O, Yamashiro M, et al. Detection of hepatocellular carcinoma by CT during arterial portography using a cone-beam CT technology: comparison with conventional CTAP. Abdom Imaging 2009; 34:502–506. [CrossRef]
15. Pung L, Ahmad M, Mueller K, et al. The role of cone-beam CT in transcatheter arterial chemoembolization for hepatocellular carcinoma: a systematic review and meta-analysis. J Vasc Interv Radiol 2017; 28:334–341. [CrossRef]
16. Iwazawa J, Ohue S, Hashimoto N, Abe H, Hamuro M, Mitani T. Detection of hepatocellular carcinoma: comparison of angiographic C-arm CT and MDCT. AJR Am J Roentgenol 2010; 195:882–887. [CrossRef]
17. Loffroy R, Lin M, Rao P, et al. Comparing the detectability of hepatocellular carcinoma by C-arm dual-phase cone-beam computed tomography during hepatic arteriography with conventional contrast-enhanced magnetic resonance imaging. Cardiovasc Intervent Radiol 2012; 35:97–104. [CrossRef]
18. Lee IJ, Chung JW, Yin YH, et al. Cone-beam CT hepatic arteriography in chemoembolization for hepatocellular carcinoma: angiographic image quality and its determining factors. J Vasc Interv Radiol 2014; 25:1369–1379. [CrossRef]
19. Miyayama S, Yamashiro M, Hashimoto M, et al. Identification of small hepatocellular carcinoma and tumor-feeding branches with cone-beam CT guidance technology during transcatheter arterial chemoembolization. J Vasc Interv Radiol 2013; 24:501–508. [CrossRef]
20. Paul J, Jacobi V, Farhang M, Bazrafshan B, Vogl TJ, Mbalisike EC. Radiation dose and image quality of X-ray volume imaging systems: cone-beam computed tomography, digital subtraction angiography and digital fluoroscopy. Eur Radiol 2013; 23:1582–1593. [CrossRef]
21. Heo SH, Jeong YY, Shin SS, et al. Apparent diffusion coefficient value of diffusion-weighted imaging for hepatocellular carcinoma: correlation with the histologic differentiation and the expression of vascular endothelial growth factor. Korean J Radiol 2010; 11:295–303. [CrossRef]
22. Park Y, Kim SH, Kim SH, et al. Gadoxetic acid (Gd-EOB-DTPA)-enhanced MRI versus gadobenate dimeglumine (Gd-BOPTA)-enhanced MRI for preoperatively detecting hepatocellular carcinoma: an initial experience. Korean J Radiol 2010; 11:433–440. [CrossRef]
23. Miyayama S, Yamashiro M, Nagai K, et al. Evaluation of tumor recurrence after superselective conventional transcatheter arterial chemoembolization for hepatocellular carcinoma: Comparison of computed tomography and gadoxetate disodium-enhanced magnetic resonance imaging. Hepatol Res 2016; 46:890–898. [CrossRef]
24. Kloeckner R, Otto G, Biesterfeld S, Oberholzer K, Dueber C, Pitton MB. MDCT versus MRI assessment of tumor response after transarterial chemoembolization for the treatment of hepatocellular carcinoma. Cardiovasc Intervent Radiol 2010; 33:532–540. [CrossRef]